

## APPENDIX B: VERIFICATION OF SUSCEPTIBILITY RESULTS

Susceptibility of C-band satellite digital television (DTV) to gated-noise interference was measured with the test system and procedures described in Part 1 [6]. These tests measured effects on DTV signal quality due to increasing levels of interference. DTV signal quality metrics collected during the tests include modulation error ratio (*MER*), pre-Viterbi bit error rate (*BER*), and post-Reed-Solomon segment error rate (*SER*).

From the point of view of interference susceptibility tests, it is essential that signal power measurements and DTV signal quality metrics be precisely defined. This appendix gives an overview of the test system, provides precise measurement definitions for signal-to-noise ratio (*SNR*), interference-to-noise ratio (*INR*), *MER*, *BER*, and *SER*, and provides some degree of validation via comparison of theoretical and measured DTV signal quality metrics for Gaussian noise degradation.

### B.1. Test System Overview

The test system was designed to inject carefully characterized interference into an operating satellite DTV receiver and measure susceptibility of the receiver with precisely defined DTV signal quality metrics. Figure B-1 is a block diagram of the test system hardware. In this figure BPF, LPF, and LNB correspond to bandpass filter, lowpass filter, and low-noise block downconverter.

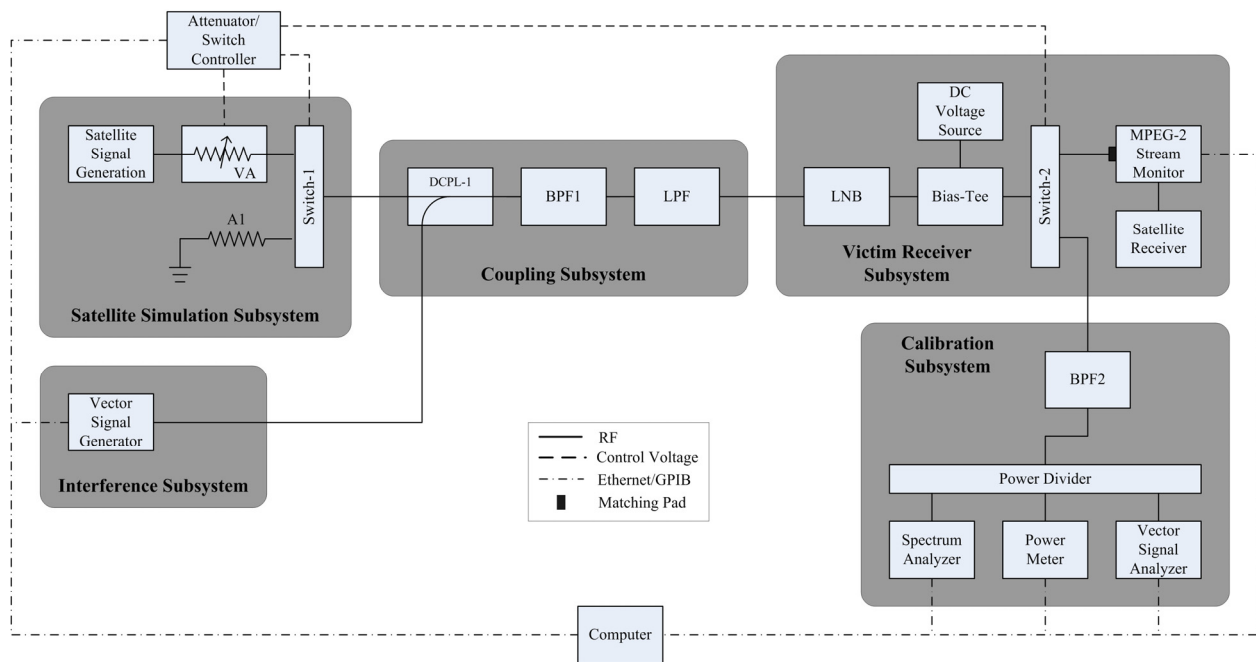


Figure B-1. Block diagram of DTV interference susceptibility test system.

The test system:

- simulated interference signals in software, so the widest range of UWB signal parameters were available for testing;
- generated interference signals with a vector signal generator (VSG), so *INR* was precisely controlled;
- characterized interference signals with a vector signal analyzer (VSA), which provided both amplitude and phase information for post-measurement analyses;
- simulated the satellite signal, so that scene content and *SNR* were controlled;
- conductively coupled signals to the satellite receiver, so uncertainties introduced by radio channel interference, attenuation, and distortion were eliminated;
- evaluated performance degradation objectively and quantitatively with DTV signal quality metrics from an MPEG-2 stream monitor;
- was completely characterized, so that its effects on the test were known;
- was under software control to eliminate procedural errors.

For this test, the operational scenario is summarized in Table B-1. Compression, modulation, and error correction schemes comply with digital video broadcast (DVB) recommendations described in *ETS 300 421* [10].

Table B-1. Operational Scenario for DTV Interference Susceptibility Tests

Transponder Center Frequency	3820 MHz
Modulation	QPSK with root-raised cosine filter ( $\alpha = 0.35$ )
Compression	MPEG-2
Data Rate	26.970353 Mbps
Symbol Rate	$R_S = 19.510468$ Mbaud
Segment Rate	$R_{seg} = 17,932$ segments/second
Reed-Solomon Error Correction	$R_{RS} = 188/204$
Convolutional Error Correction	$R_{conv} = 3/4, K = 7$
Interleaving	Depth = 12 bytes
Signal-to-Noise Ratio	{8.5, 11.5, 14.5} dB

## B.2. Signal Calibration

At the beginning of each test, the system was calibrated to ensure that all hardware was operating properly and *SNR* and *INR* were correct. Figure B-2 provides a simplified model of the four calibration measurements: ( $m_1$ ) VSA noise, ( $m_2$ ) combined system noise and VSA noise, ( $m_3$ ) combined DTV signal, system noise, and VSA noise, and ( $m_4$ ) combined interference, system noise, and VSA noise. For these measurements, DTV signal power was set to a level corresponding to the appropriate *SNR*, the interfering signal power was set to a level that produced an accurate VSA measurement, and a 36-MHz VSA span was used. The satellite signal path (SSP) and interference signal path (ISP) were characterized in Appendix F of Part 1.

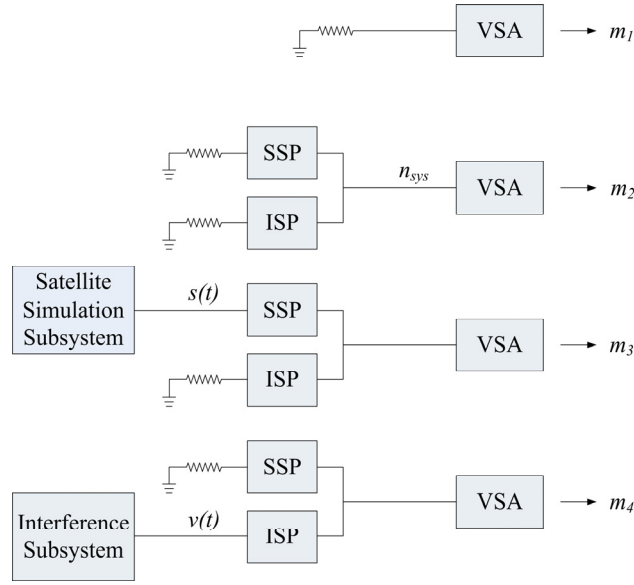


Figure B-2. Block diagrams for calibration measurements.

The following equations define these measurements

$$m_1(t) = n_{vsa}(t) + n_0(t)$$

$$m_2(t) = n_{sys}(t) + n_{vsa}(t)$$

$$m_3(t) = G_{SSP} s(t) + n_{sys}(t) + n_{vsa}(t)$$

$$m_4(t) = G_{ISP} v(t) + n_{sys}(t) + n_{vsa}(t)$$

where  $n_{vsa}(t)$  is the internal noise of the VSA instrument,  $n_0(t)$  is thermal noise,  $n_{sys}(t)$  is the system noise,  $s(t)$  is the satellite signal,  $v(t)$  is the interference signal, and  $G_{SSP}$  and  $G_{ISP}$  are gains of SSP and ISP, respectively. The noise analysis was simplified by assuming the gain of the VSA to be one; this is justified because gain of the VSA is divided out in the power ratio calculations.

Measurement results were then band-limited in post-measurement processing by the victim receiver RRC filter

$$P_k = \left\langle |m_k(t) * h_{rrc}(t)|^2 \right\rangle$$

where  $k$  is the measurement index,  $h_{rrc}(t)$  is the impulse response of the victim receiver RRC filter,  $\langle \rangle$  is the time-average operator, and  $*$  is the convolutional operator. Power estimates were derived from approximately 2.8 milliseconds of data, i.e.,  $2^{17} = 131,072$  samples.

Power of the system noise ( $P_N$ ), satellite signal ( $P_S$ ), and interference signal ( $P_I$ ) are calculated as

$$P_N \approx P_2 - P_1$$

$$P_S = P_3 - P_2$$

$$P_I = P_4 - P_2 \quad ,$$

where  $P_N$  is a good estimate because  $n_{\text{sys}}(t) \gg n_0(t)$ .

Finally,  $SNR$  and  $INR$  are computed as

$$SNR = \frac{P_S}{P_N}$$

$$INR = \frac{P_I}{P_N} \quad .$$

Example calculations are provided in the validation portion of this appendix (see Table B-3).

### B.3. Measured DTV Signal Quality

The MPEG-2 stream monitor was used to measure DTV signal quality. DTV signal quality metrics and their reference points within the receiver include  $MER$  and  $BER$  at the output of the quadrature demodulator, or equivalently at the input of the Viterbi decoder, and  $SER$  at the output of the Reed-Solomon (RS) decoder.

During the test, the following procedure was followed at each discrete interference level:

1. Interference was turned off and the receiver was allowed to acquire and demodulate the desired satellite signal in the absence of interference for 20 seconds.
2. Interference was applied for approximately 200 seconds.
3.  $MER$ ,  $BER$ , cumulative transport error flag ( $TEF$ ), and UTC time were sampled during the time of interference exposure at about 3 times per second and written to a data file.

DTV signal quality metrics were acquired with coarse and fine interference-level resolution. For coarse resolution, interference level was increased in 2-dB steps, beginning at a level that had negligible effect on DTV signal quality and ending where  $SER$  was in excess of 0.1. Fine-resolution acquisition began 2 dB below the level where the first  $TEF$  occurred during coarse-resolution acquisition and interference was incremented in 0.1-dB steps until 0.1  $SER$  was again achieved.

### B.3.1. MER

Measured *MER* is defined as

$$MER = 10 \log_{10} \left( \frac{\sum_{n=1}^N (I_n^2 + Q_n^2)}{\sum_{n=1}^N (\delta I_n^2 + \delta Q_n^2)} \right),$$

where  $I_n$  and  $Q_n$  are the ideal in- and quadrature-phase samples of the demodulated signal,  $\delta I$  and  $\delta Q$  are the error between actual and ideal samples, and  $N$  is the number of samples used for estimation. The MPEG-2 stream monitor utilized in this experiment derives *MER* from 512 samples collected at a rate of approximately 25 Hz.

### B.3.2. BER

Measured pre-Viterbi bit error rate is defined as

$$BER = \frac{\text{bit error count}}{\text{bit count}}.$$

The MPEG-2 stream monitor estimates *BER* with the circuit illustrated in Figure B-3. This circuit compares received bits to the estimated transmit bits. *BER* measurements use  $2^{26} = 67,108,864$  bits which provide good precision to approximately  $7 \cdot 10^{-5}$  *BER* assuming 100 errors are needed.

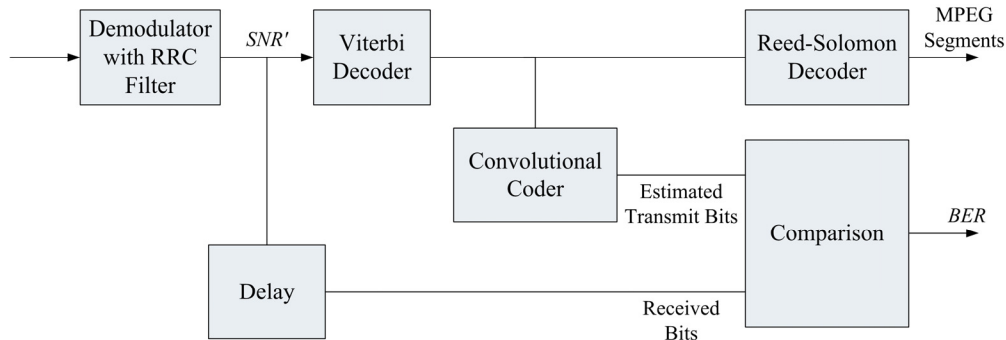


Figure B-3. *BER* estimation circuit used by MPEG-2 stream monitor.

Figure B-4 displays simulation results for the *BER* estimation circuit, where no interference was present. Good agreement was found for  $SNR' > 4.5$  dB corresponding to  $BER < 0.05$ , where  $SNR'$  is referenced to the output of the demodulator. Poor agreement at lower  $SNR'$  was due to errors in the estimated transmit bits.

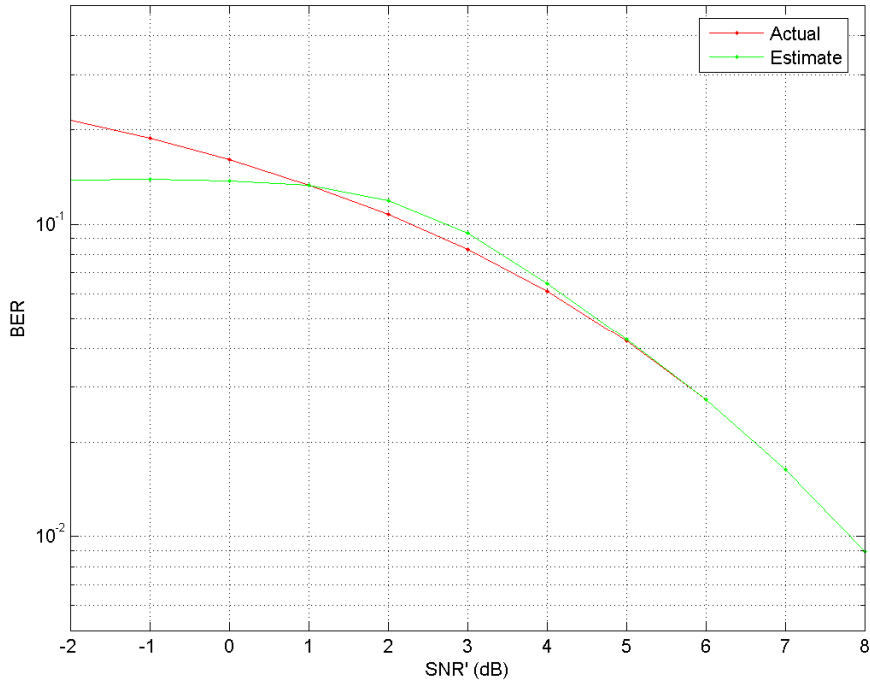


Figure B-4. Simulation of *BER* estimation circuit used by MPEG-2 stream monitor.

### B.3.3. *SER*

Measured *SER* is defined by

$$SER = \frac{\text{segment error count}}{\text{segment count}} = \frac{TEF(t_2) - TEF(t_1)}{(t_2 - t_1)R_{seg}},$$

where  $TEF(t_k)$  is the cumulative number of segment errors at UTC time  $t_k$  and  $R_{seg}$  is the number of segments per second specified by the DTV operational scenario. Measured *SER* was computed from approximately 200 seconds of data. During this time period, approximately 3.6 million segments were transmitted. Each segment is considered to be an independent susceptibility trial.

Satellite and interference signals were not without systematic uncertainty. More specifically, sinusoidal variations of approximately 0.1-dB peak-to-peak with periods of 20 – 50 minutes were measured in signal amplitudes with a power meter after the LNB. Subsequent *SER* fluctuations were approximately an order of magnitude, which is explained by the high sensitivity of *SER* to change in signal-to-noise ratio (see Table B-2). This *SER* fluctuation is only evident during long measurement periods when interference is either absent or has negligible effect on *SER*. For the interference tests considered in this report, the 0.1-dB increase in interference power every 220 seconds increased *SER* at a rate that rendered the *SER* systematic fluctuations indistinguishable.

## B.4. Theoretical DTV Signal Quality for Gaussian Noise Degradation

This section provides theoretical expressions of  $MER$ ,  $BER$ , and  $SER$  for Gaussian noise degradation. For a Gaussian noise radio environment, degradation is predictable from the signal-to-noise ratio at the output of the demodulator ( $SNR'$ ).

### B.4.1. $MER$

For Gaussian noise degradation, theoretical  $MER$  is equivalent to  $SNR'$  in dB, that is

$$MER = 10 \log(SNR') \quad .$$

### B.4.2. $BER$

Theoretical probability of a bit error for QPSK, comparable to measured  $BER$ , is computed as

$$P_{QPSK} = Q(\sqrt{SNR'}) \quad ,$$

where  $Q$  represents the  $Q$ -function defined as

$$Q(z) = \frac{1}{2\pi} \int_z^{\infty} \exp\left(-\frac{\xi^2}{2}\right) d\xi \quad .$$

### B.4.3. $SER$

Probability of post-Viterbi bit error for QPSK is upper bounded by

$$P_{conv} \leq \frac{1}{K} \sum_{d=d_{free}}^{\infty} w(d) Q(\sqrt{d \cdot SNR'}) \quad ,$$

where constraint length  $K$  is specified by the operational scenario,  $d_{free}$  is the free distance of the code, and  $w(d)$  are the code weights.

Theoretical calculation of  $SER$  requires converting  $P_{conv}$  to  $P_{byte}$ , i.e., the probability of a byte error. The conversion factor can be determined mathematically with the assumption of independent bit errors [11]; however, if more accuracy is desired the effects of correlated bit errors, caused by the Viterbi algorithm, can be simulated. Simulations of Gaussian noise degradation near the  $SNR'$  required for  $P_{RS} = 10^{-4}$  have shown a probability of a byte error approximately equal to three times the probability of a bit error, i.e.,  $P_{byte} \approx 3P_{conv}$ .

For the RS scheme specified in Table B-1, a segment error occurs when more than  $(204 - 188)/2$  or 8 byte errors occur in a single segment. Hence, if post-Viterbi byte errors are independent,  $P_{byte}$  is small, and the number of bytes per segment is large, then the upper bound of the probability of a post RS segment error can be estimated by

$$P_{RS} = P(m > M) \leq 1 - \sum_{l=0}^M \frac{\lambda^l}{l!} e^{-\lambda} \quad ,$$

where  $M = 8$  and  $\lambda = 204P_{byte}$  for the RS(204,188) code.

Figure B-5 shows  $P_{QPSK}$ ,  $P_{conv}$ , and  $P_{RS}$  as a function of  $SNR'$ . Table B-2 provides  $P_{QPSK}$  and  $P_{RS}$  at various  $SNR'$  near the threshold of visibility, i.e.,  $P_{RS} = 10^{-4}$ . Notice that  $P_{RS}$  is sensitive to changes in  $SNR'$ , varying as much as an order of magnitude for each 0.1-dB increment in  $SNR'$ . In contrast,  $P_{QPSK}$  is relatively insensitive. Such differences between  $P_{QPSK}$  and  $P_{RS}$  are attributed to the forward error correction (FEC).

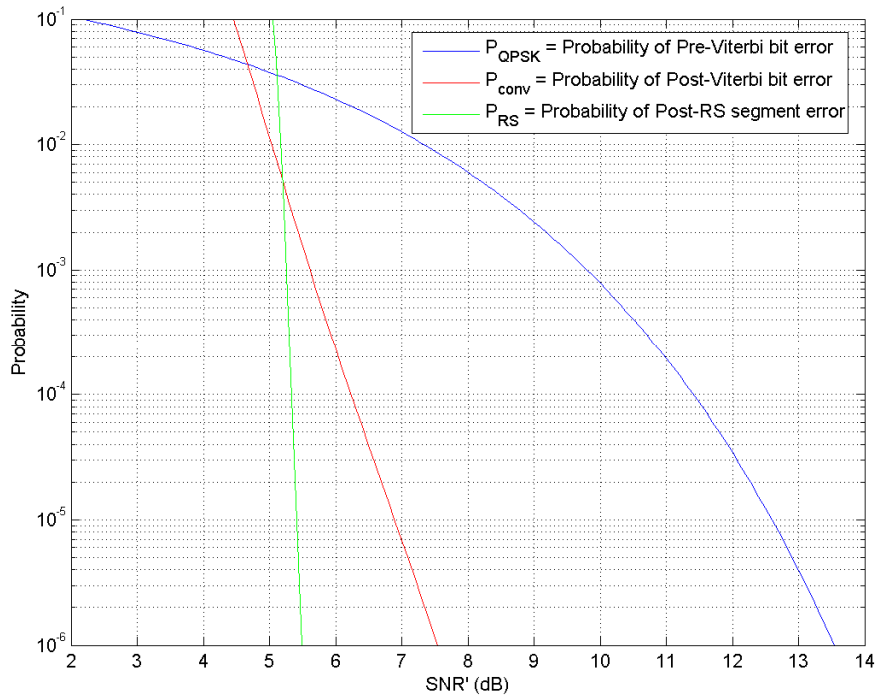


Figure B-5. Theoretical DTV receiver performance versus  $SNR'$ .

Table B-2. Probability of Pre-Viterbi Bit Error and Post-RS Segment Error Near TOV

$SNR'$ (dB)	$P_{QPSK}$	$P_{RS}$
5.0	0.038	0.27
5.1	0.036	0.046
5.2	0.034	0.0045
5.3	0.033	0.00029
5.4	0.031	0.000014

## B.5. Validation of Measured DTV Quality Metrics for Gaussian Noise Degradation

In this section, some degree of validation is accomplished by comparing theoretical predictions to measured DTV quality metrics for Gaussian noise degradation. Two scenarios are evaluated: (1) *BER* versus *SNR* in the absence of interference, and (2) *BER* and *SER* versus *INR* for a DTV receiver exposed to continuous noise interference. It is important to understand that results in this subsection relate to Gaussian noise degradation and cannot be generalized without further research.

### B.5.1. *BER* as a Function of *SNR* in the Absence of Interference

The test system was set up as shown in Figure B-1, except the interference signal path was terminated. *SNR*, *BER*, and *SER* were measured (as described in Sections B.2 and B.3) at various satellite signal powers. Figure B-6 shows measured *BER* and theoretical  $P_{QPSK}$  versus *SNR*.

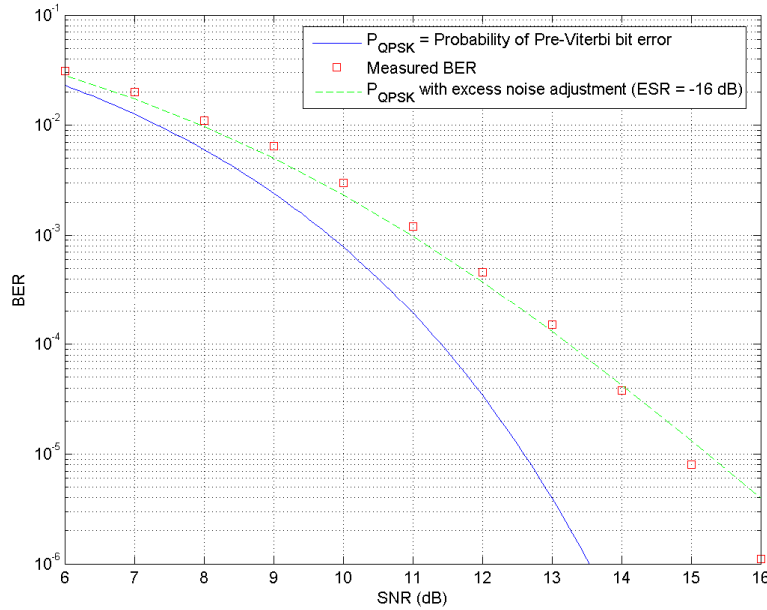


Figure B-6. Theoretical versus measured bit error rate performance of a DTV receiver.

Presumably, the primary difference between theory and measurement was due to distortions introduced by imperfect demodulation that effectively reduced the signal-to-noise ratio. Good agreement with measured *BER* was achieved when an excess noise term, proportional to the average power of the satellite signal, was used to model demodulator imperfections. More specifically, at the output of the demodulator

$$SNR' = \frac{P_s}{P_N + P_\epsilon} = \frac{SNR}{1 + ESR \cdot SNR} \quad , \quad (B-1)$$

where  $P_\epsilon$  is the average power of the excess noise and excess-noise-to-signal ratio was determined empirically as  $ESR = P_\epsilon / P_S = -16$  dB. Using this model,  $SNR = \{9, 12, 15\}$  dB measured during the DTV susceptibility test corresponds to  $SNR' = \{8.2, 10.5, 12.5\}$  dB.

### B.5.2. BER and SER as a Function of INR for Gaussian-Noise Interference

In this subsection, an “effective signal-to-noise ratio” concept is developed to validate the GN-01 measurements. This concept is based on the assumption that receiver noise, excess noise, and GN-01 interference are all Gaussian noise processes. Theoretical expressions provided in Section B.4 are applicable since the addition of these noise processes results in a Gaussian noise process with an average power equal to the sum of its constituents. Hence, in the case of GN-01, the effective signal-to-noise ratio at the output of the demodulator is expressed as

$$SNR'_{eff} = \frac{P_S}{P_N + P_I + P_\epsilon} = \frac{SNR}{1 + INR + ESR \cdot SNR}$$

Figures B-7 and B-8 provide theoretical versus measured BER and SER, respectively, for a DTV receiver operating at the different SNRs and exposed to a range of Gaussian noise interference levels. Table B-3 provides theoretical and measured test results for Gaussian noise interference that caused degradation at the TOV. Calibration measurements with the VSA provided  $P_1, P_2, P_3,$  and  $P_4$ . These measurements were used to compute  $P_S, P_I, SNR,$  and  $INR$ . Interestingly,  $P_S / P_4$ , which corresponds to the ratio of signal power to the combined power of interference and system noise, was approximately 5.5 dB in all cases. In general, theoretical results using the  $SNR'_{eff}$  model demonstrated good agreement with measured data.

Table B-3. Signal Powers at the TOV for Gaussian Noise Interference

Calibration Measurements			Susceptibility Test Results					Theoretical Results
$P_2$ (dBm)	$P_3$ (dBm)	$P_4$ (dBm)	$P_S$ (dBm)	$P_I$ (dBm)	$P_S/P_4$ (dB)	$SNR$ (dB)	$INR_{TOV}$ (dB)	$INR_{TOV}$ (dB)
-47.8	-38.4	-44.4	-38.9	-47.1	5.5	8.9	0.7	0.5
-47.7	-35.4	-41.2	-35.7	-42.3	5.5	12.0	5.4	5.1
-47.8	-32.6	-38.1	-32.7	-38.6	5.4	15.0	9.2	8.7

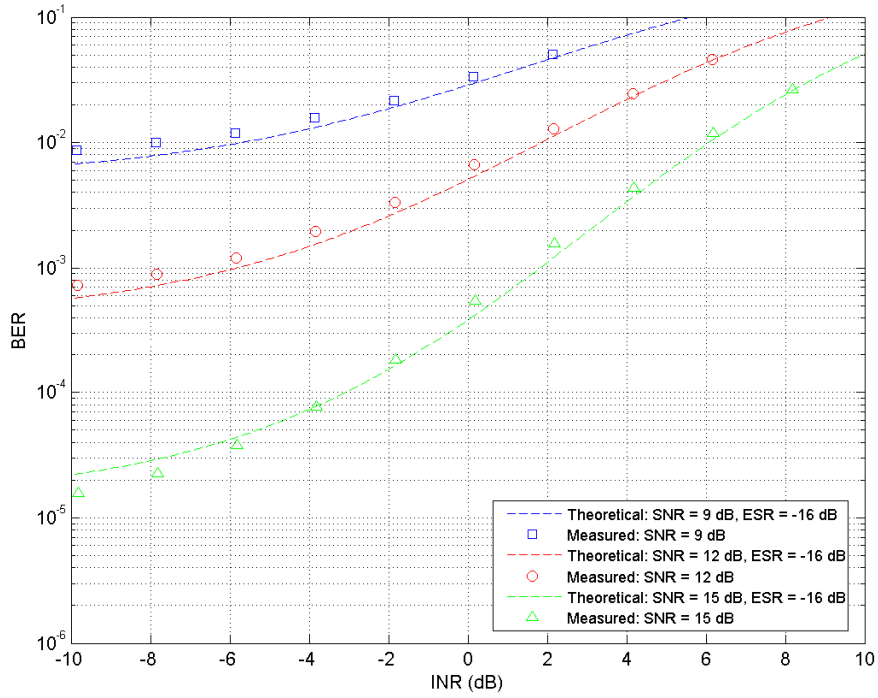


Figure B-7. Theoretical and measured *BER* for Gaussian noise interference.

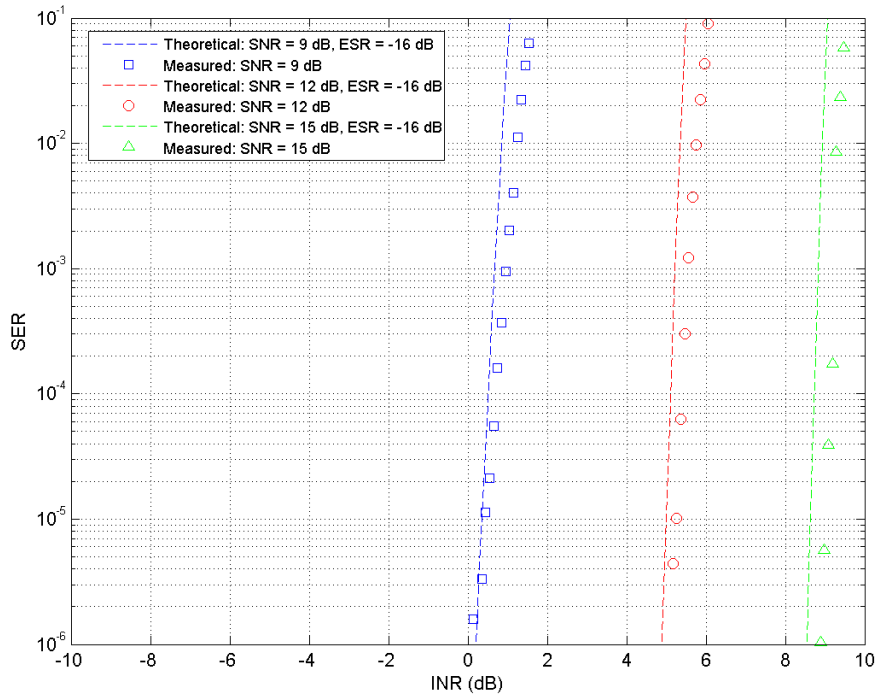


Figure B-8. Theoretical and measured *SER* for Gaussian noise interference.